Sensors and Actuators B 245 (2017) 615–621

Contents lists available at ScienceDirect

Sensors and Actuators B: Chemical

journal homepage: www.elsevier.com/locate/snb

Real-time *in vitro* detection of cellular H_2O_2 under camptothecin stress using horseradish peroxidase, ionic liquid, and carbon nanotube-modified carbon fiber ultramicroelectrode

Qiong-Qiong Ren[a], Jing Wu[b], Wen-Chao Zhang[a], Chang Wang[a], Xin Qin[a], Guo-Chang Liu[c], Zhen-Xin Li[a,*], Yi Yu[a,*]

[a] School of Biomedical Engineering, Xinxiang Medical University, China
[b] Institute of Lung and Molecular Therapy, Xinxiang Medical University, China
[c] Britton Chance Center for Biomedical Photonics at Wuhan National Laboratory for Optoelectronics-Hubei Bioinformatics and Molecular Imaging Key Laboratory, Department of Biomedical Engineering, College of Life Science and Technology, Huazhong University of Science and Technology, Wuhan 430074, China

ARTICLE INFO

Article history:
Received 12 September 2016
Received in revised form 30 January 2017
Accepted 1 February 2017
Available online 1 February 2017

Keywords:
Hydrogen peroxide
Single-walled carbon nanotubes
Horseradish peroxidase
Room-temperature ionic liquids
Carbon fiber
Real-time monitoring

ABSTRACT

Single-walled carbon nanotubes (SWCNTs), horseradish peroxidase (HRP), and 1-butyl-3-methylimidazolium tetrafluoroborate (BMIM·BF_4) were employed to construct a cellular H_2O_2 sensor based on direct electron transfer. At a working potential of −0.35 V, HRP-BMIM·BF_4/SWCNTs/CFUME showed a dynamic range of up to 10.2 μM with a low detection limit of 0.13 μM (S/N = 3) and a high sensitivity of 4.25 A/M cm^2. The apparent Michaelis-Menten constant ($K_{m,app}$) was estimated to be as low as 15.4 μM, which suggested that HRP molecules entrapped in the BMIM·BF_4 and SWCNTs immobilized at the carbon fiber ultramicroelectrode maintained a very high affinity. Because of the extremely small dimension and low working potential, HRP-BMIM·BF_4/SWCNTs/CFUME enabled direct amperometric real-time monitoring of H_2O_2 in HeLa cells treated with the anticancer drug, camptothecin, without requiring complex data processing and extra surface coatings to prevent interference. HRP-BMIM·BF_4/SWCNTs/CFUME testing clearly showed that the H_2O_2 level significantly increased in HeLa cells under camptothecin stress. When HeLa cells were cultured in medium without camptothecin, the H_2O_2 level remained stable during the whole measurement process. These results indicate that HRP-BMIM·BF_4/SWCNTs/CFUME could be a powerful tool for real-time investigation of cellular H_2O_2 level, especially under anticancer drug stress. This method could provide in-depth insights regarding the occurrence, development, and apoptosis of tumors.

1. Introduction

Mounting evidence suggests that compared to normal cells, hydrogen peroxide (H_2O_2) levels are greatly increased in many types of cancer cells [1]. H_2O_2 helps cancer cells to infiltrate and metastasize to other tissues [2] and is an important signal molecule regulating the entire process of tumor cell survival, proliferation, and apoptosis [3]. As cancer cells are under increased intrinsic oxidative stress, they are more vulnerable to further oxidative insults induced by H_2O_2-generating agents or by compounds that abrogate the key antioxidant systems in cells. Chemotherapy drugs widely used in the clinic such as paclitaxel, arsenic trioxide, luteolin, and doxorubicin increase the intracellular H_2O_2 content directly or indirectly to induce apoptosis [4].

The World Health Organization (WHO) reported that the incidence of death from cancer was 8.2 million people in 2012. Effective prevention and control of cancer depend on an in-depth understanding of the occurrence, development, and apoptosis of tumors. Understanding the changes in H_2O_2 levels during apoptosis of cancer cells induced by drugs is important in for chemical control of cancer.

Various techniques have been developed for analysis of cellular H_2O_2, including chemiluminescence [5], colorimetry [6], and fluorescence [7]. However, these methods are difficult for *in vivo* and *in vitro* real-time and dynamic studies of H_2O_2 because they require tracers or instable chemical probes. In contrast, electro-

* Correspondence to: Department of Biomedical Engineering, Xinxiang, Henan, China.
E-mail addresses: xxmu2008lzx@163.com (Z.-X. Li), xxmu2010yy@163.com (Y. Yu).

http://dx.doi.org/10.1016/j.snb.2017.02.001
0925-4005/

chemical techniques are more suitable for continuous real-time H_2O_2 measurement because of their simplicity, rapidity, and label-free detection capability. Moreover, electrochemical sensor can be made extremely small such that high spatial resolution can be achieved [8].

Carbon fiber ultramicroelectrodes (CFUMEs) are an ideal tool for electrochemical monitoring of biological samples because of their favorable biocompatibility, easy fabrication, good electron transfer properties, and extremely small dimensions, which could match the biological microenvironment in cells or tissues with minimal perturbation or damage [9]. Single-walled carbon nanotubes (SWCNTs) present a high surface-to-volume ratio, high conductivity, and electrocatalytic activity, which increases the sensitivity of sensors by promoting electron transfer to biomolecules and inhibiting surface fouling by biomolecules [10]. There are several catalytic enzymes for heme proteins such as catalase (CAT), cytochrome c (Cyt c), horseradish peroxidase (HRP), microperoxidase (Mp), and myoglobin (Mb). HRP is one of the heme enzymes, which contain iron-centered porphyrins as their prosthetic group and easily undergo oxidation and reduction over a wide range of potentials [11]. HRP based electrodes have high sensitivity for H_2O_2 [12]. Room-temperature ionic liquids (RTILs) are ion compounds that remain in the liquid state at room temperature. RTILs possess unique properties such as high thermal stability and viscosity, good conductivity, and solubility, which make them novel solvent (electrolyte) systems with great potential in electrochemical applications [13]. The direct electron-transfer reaction between redox proteins or enzymes and RTIL-based composite electrodes has received considerable attention in recent years. These composite materials provide a suitable microenvironment to maintain the enzymatic activity and facilitate electron-transfer rate between the active center of redox proteins or enzymes and the underlying electrode [14]. However, not all RTILs are suitable for biocatalysis. Park and Kazlauska [15] reported that enzymes are usually active in RTILs that contain BF_4^-, PF_6^-, and Ntf_2^- anions. In this study, 1-butyl-3-methylimidazolium tetrafluoroborate (BMIM·BF_4), which is soluble in water, was chosen to fabricate the HRP-RTIL composites.

In this study, a step-by-step immobilization of HRP-BMIM·BF_4 and SWCNTs on the surface of CFUMEs was performed for real-time *in vitro* detection of cellular H_2O_2. The HRP-BMIM·BF_4/SWCNTs/CFUMEs were electrochemically characterized and their sensitivity and selectivity were investigated. HeLa cells, which generate H_2O_2 endogenously under stimulation by ascorbic acid (AA) [16], were chosen as model cells to demonstrate the electrochemical detection ability of the HRP-BMIM·BF_4/SWCNTs/CFUMEs. The change in cellular H_2O_2 levels caused by camptothecin stress, which induces cancer cell apoptosis, was also measured.

2. Materials and methods

2.1. Chemicals

HeLa cells were from the China Center for Type Culture Collection (CCTCC, Wuhan, China). Camptothecin, glutathione (GSH), glucose (GLU), ascorbic acid (AA), dopamine (DA), glycine (Gly), uric acid (UA), and hexadecyltrimethyl ammonium bromide (CTAB) were purchased from Sigma-Aldrich (St Louis, MO, USA). SWCNTs (purity >95 wt%, outer diameter of 10–20 nm, length of 5–15 μm) were bought from Nanoport (Shenzhen, China) and used as received. HRP and 1-butyl-3-methylimidazolium tetrafluoroborate were purchased from Aladdin (Shanghai, China). H_2O_2 (30 wt%), glucose, and all other reagents were purchased from Sinopharm (Shanghai, China). Carbon fiber (diameter 7 μm) was purchased from Goodfellow Co. (Oxford, UK). Borosilicate glass capillaries (inner diameter 0.9 mm, outer diameter 1.1 mm) were purchased from West China Medical Instrument Inc. (Chengdu, China). All solutions used in the experiments were prepared with deionized water (18 MΩ cm, Millipore, Billerica, MA, USA). To eliminate dissolved oxygen, the solutions were purged with high purity argon (99.99%, Minghui Gas Inc., Wuhan, China) for 20 min. An argon atmosphere was maintained over the solutions during the anaerobic electrochemical investigations.

2.2. Apparatus

All electrochemical measurements were performed with a three-electrode system, including CFUME, Pt wire (diameter 0.1 mm), and AgCl coated Ag wire (diameter 0.1 mm), as working, counter, and reference electrodes, respectively. A computer-controlled CHI660A electrochemical workstation was used for all electrochemical experiments. A scanning electron microscope (SEM) (Nova 450, FEI Inc. Holland) was used to investigate the morphology of CFUMEs.

2.3. Fabrication and modification of CFUMEs

CFUMEs were fabricated as previously described [10]. In brief, a glass capillary was pulled to obtain a tip size of 20 μm. A carbon fiber was glued to a copper wire using conducting silver paste and the carbon fiber-copper wire was carefully inserted through the tip from the other end of the pulled glass capillary. Approximately 1 cm of the carbon fiber was exposed from the tip. Then, the copper wire was fixed with epoxy in the capillary. The tip of capillary was fused on a flame to seal the carbon fiber. The length of the protruded carbon fiber was cut to 300 μm with a scalpel under the inverted microscope. CFUMEs were then ultrasonically rinsed in acetone and double distilled water sequentially. Then, the CFUMEs were electrochemically activated by potential cycling in PBS (pH = 7.0) in a potential range from −0.2 to +1.2 V at 100 mV/s until stable cyclic voltammograms were obtained.

SWCNTs (3 mg) were dispersed in 1 mL of CTAB (10 mg/mL), and the mixture was agitated in an ultrasonic bath for 1 h to obtain a homogeneous black suspension. CFUME was soaked in 1 mL of the SWCNTs-CTAB mixture under an infrared lamp until the solvent was completely evaporated. HRP-BMIM·BF_4/SWCNTs/CFUME was fabricated by soaking SWCNTs/CFUME in 10 mg/mL HRP (dissolved in 5% BMIM·BF_4 (v/v)) for 12 h at 4 °C. HRP/SWCNTs/CFUME and HRP/CFUME were prepared accordingly. HRP was dissolved in PBS to fabricate the HRP/SWCNTs/CFUME.

2.4. Cell culture

HeLa cells (cervical cancer cell line) were cultured in RPMI-1640 medium containing 10% fetal bovine serum (Gibco, Carlsbad, CA, USA) and 100 U/mL penicillin-streptomycin at 37 °C with 5% CO_2 in water vapor-saturated air atmosphere. HeLa cells growing in 25-cm^2 cell culture flasks were subcultured in 20-mm dishes for 24 h for electrochemical experiments. The culture medium was removed and the cells were washed three times with PBS (136.7 mM NaCl, 2.7 mM KCl, 9.7 mM Na_2HPO_4, 1.5 mM KH_2PO_4, pH 7.4), and then 1 mL of PBS containing 50 mM glucose was added for electrochemical measurements.

2.5. Electrochemical measurements of H_2O_2 released from HeLa cells

Amperometric detection of the release of H_2O_2 from HeLa cells was performed with HRP-BMIM·BF_4/SWCNTs/CFUME, which were placed in the cells that adhered to the dish. After a steady state

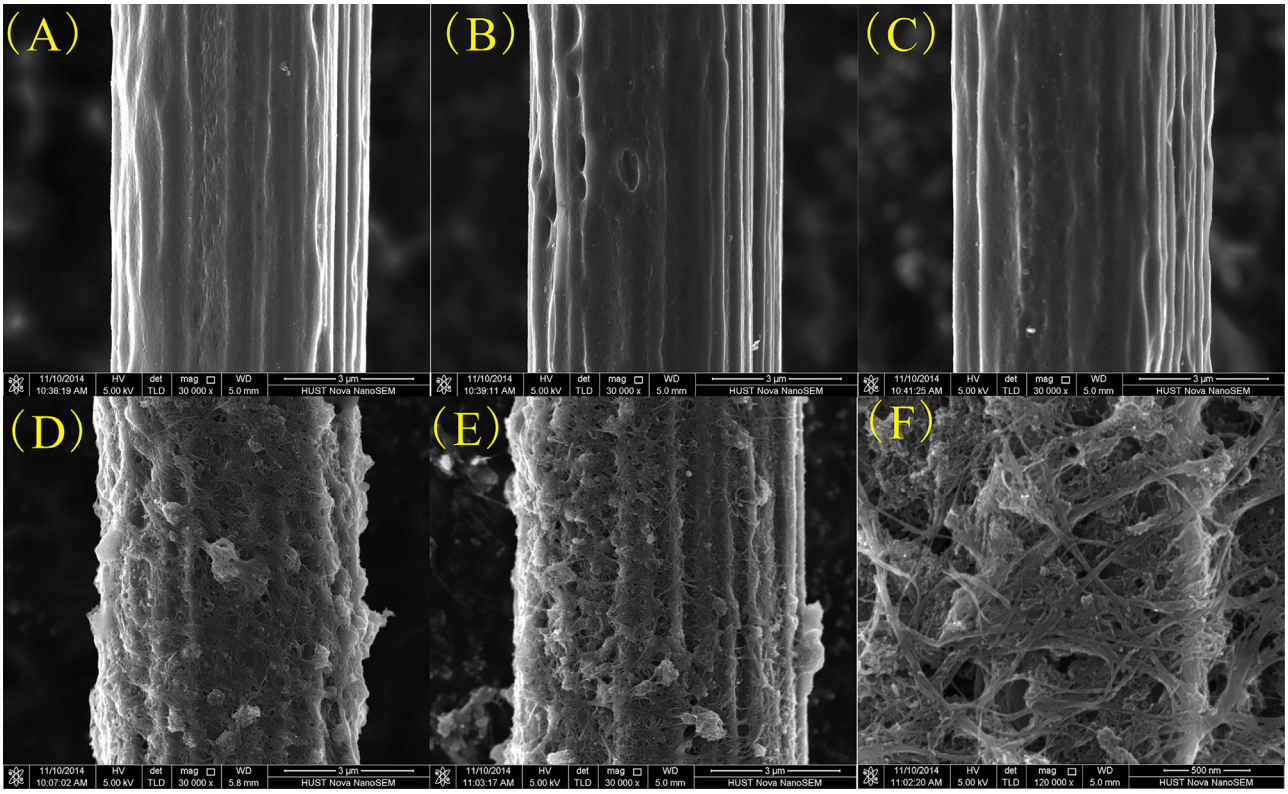

Fig. 1. SEM of CFUME (A), HRP/CFUME (B), HRP-BMIM·BF_4/CFUME (C), SWCNTs/CFUME (D), HRP/SWCNTs/CFUME (E), and the tip of HRP-BMIM·BF_4/SWCNTs/CFUME (F).

background was obtained, 5 μM AA or camptothecin was injected into the buffer, and the amperometric responses to the electrocatalytic reduction of H_2O_2 released from the cells was recorded under an applied potential of −0.35 V.

3. Results and discussion

3.1. SEM characterization

The surface morphologies of bare CFUME (A), HRP/CFUME (B), HRP/BMIM·BF_4/CFUME (C), SWCNTs/CFUME (D), HRP/SWCNTs/CFUME (E), and the tip of HRP-BMIM·BF_4/SWCNTs/CFUME (F) were investigated by SEM. Fig. 1 shows the bare CFUME surface, which has humps and concaves on the scale of 1 μm. The flame-etching treatment in the capillary tip sealing step caused this slightly rough morphology of the bare CFUME [17]. As shown in Fig. 1B and C, the HRP/CFUME and HRP-BMIM·BF_4/CFUME surfaces showed negligible differences compared to the bare CFUME. In comparison, the SWCNTs/CFUME surface was decorated with SWCNTs, which showed as tangled SWCNTs, as depicted in Fig. 1D. This morphology suggests that SWCNTs immobilized on the CFUME surface would greatly increase the specific surface area for HRP and BMIM·BF_4 immobilization. After soaking of SWCNTs/CFUME in BMIM·BF_4 or HRP (dissolved in 5% BMIM·BF_4 (v/v)), there was no obvious difference in the morphology of the surface because of the small amount of HRP or BMIM·BF_4 adsorbed in the vacant spaces of the SWCNT sheets.

3.2. Electrochemical characterization of HRP-BMIM·BF_4/SWCNTs/CFUME

The electrochemical behavior of the immobilized HRP was characterized by cyclic voltammetry in 0.01 M deoxygenated PBS (pH = 7.0). The CVs of bare CFUME (a), HRP/CFUME (b), HRP-BMIM·BF_4/CFUME (c), SWCNTs/CFUME (d), BMIM·BF_4/SWCNTs/CFUME (e), HRP/SWCNTs/CFUME (f), and HRP-BMIM·BF_4/SWCNTs/CFUME (g) is presented in Fig. 2. No obvious redox peaks were identified for the bare CFUME, HRP/CFUME, HRP-BMIM·BF_4/CFUME, SWCNTs/CFUME, and BMIM·BF_4/SWCNTs/CFUME in the potential range of −0.8–0.2 V. This can be explained by the fact that HRP could hardly be absorbed on the bare CFUME without the aid of SWCNTs. After the SWCNT-modified CFUME was inserted in the HRP solution for 12 h, a pair of small redox peaks with an anodic peak potential (E_{pa}) of −0.25 V and a cathodic peak potential (E_{pc}) of −0.35 V were observed. In contrast, after incorporation of BMIM·BF_4 in the HRP solution, the redox peaks obviously increased at the same potentials. The formal potential ($E^{0'}$), obtained by averaging

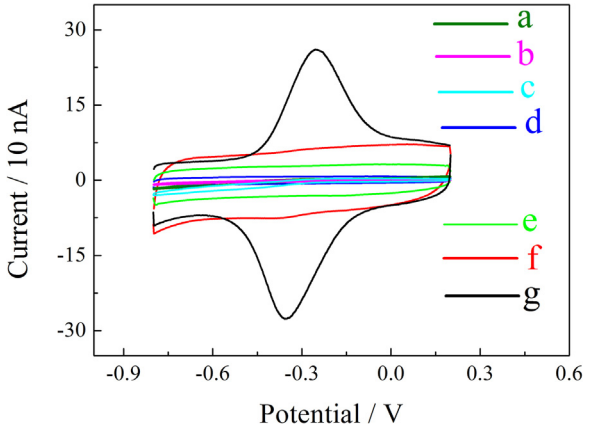

Fig. 2. Cyclic voltammograms of CFUME (a), HRP/CFUME (b), HRP-BMIM·BF_4/CFUME (c), SWCNTs/CFUME (d), BMIM·BF_4/SWCNTs/CFUME (e), HRP/SWCNTs/CFUME (f), and HRP-BMIM·BF_4/SWCNTs/CFUME (g) in 0.01 M deoxygenated PBS, pH 7.0, at a scan rate of 100 mV/s.

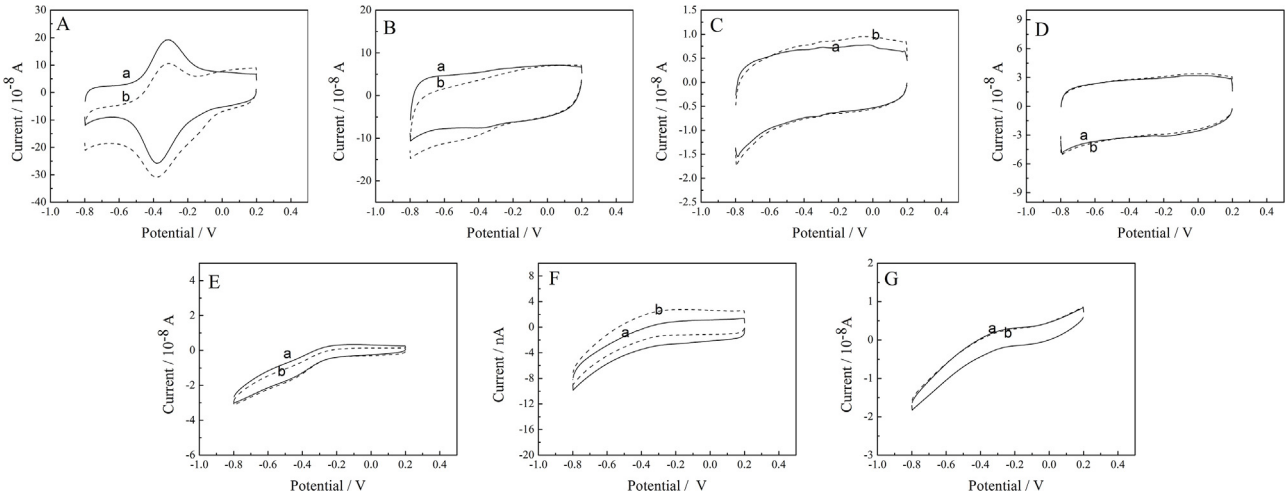

Fig. 3. Cyclic voltammograms of the HRP-BMIM·BF_4/SWCNTs/CFUME (A), HRP/SWCNTs/CFUME (B), BMIM·BF_4/SWCNTs/CFUME (C), SWCNTs/CFUME (D), HRP-BMIM·BF_4/CFUME (E), HRP/CFUME (F), and CFUME (G) in 0.01 M deoxygenated PBS, pH 7.0, in the absence of H_2O_2 (a) and presence of 30 μM H_2O_2 (b). Scan rate = 100 mV/s.

potential values of the anodic and cathodic peaks (E_{pa} and E_{pc}), was −0.3 V with a peak potential separation of approximately 100 mV, indicating a quasi-reversible process [18]. The reversible redox peaks resulted from the FeIII/FeII couple of the heme proteins. This is substantiated by comparing the observed values to those for the heme protein formal potentials measured in solution [19]. The enlarged interface area and good conductivity of SWCNTs, which provide many efficient paths for direct electron conduction between HRP and the CFUME, enhanced the current signals of HRP/SWCNTs/CFUME and HRP-BMIM·BF_4/SWCNTs/CFUME [20]. Compared with HRP/SWCNTs/CFUME, the BMIM·BF_4 entrapped in the three-dimensional HRP-BMIM·BF_4/SWCNTs/CFUME could provide a favorable microenvironment to facilitate electron transfer between the HRP and CFUME [21].

3.3. *Electrocatalytic reduction of H_2O_2 on HRP-BMIM·BF_4/SWCNTs/CFUME*

CVs were initially used to investigate the electrocatalytic properties of the modified microelectrodes for H_2O_2 reduction. The response to the presence and absence of 30 μM H_2O_2 on HRP-BMIM·BF_4/SWCNTs/CFUME, HRP/SWCNTs/CFUME, BMIM·BF_4/SWCNTs/CFUME, SWCNTs/CFUME, HRP-BMIN·BF_4/CFUME, HRP/CFUME, and CFUME were recorded in deoxygenated 10 mM pH 7.0 PBS, as shown in Fig. 3. Upon addition of H_2O_2, the cathodic currents of HRP-BMIM·BF_4/SWCNTs/CFUME and HRP/SWCNTs/CFUME showed an obvious increase, indicating that H_2O_2 was catalytically reduced on the electrodes. Additionally, HRP-Fe(II) was oxidized to HRP-Fe(III). BMIM·BF_4/SWCNTs/CFUME, SWCNTs/CFUME, HRP-BMIN·BF_4/CFUME, HRP/CFUME, and CFUME showed negligible changes, suggesting that these five electrodes provided almost no electrocatalysis to reduce H_2O_2. Compared to BMIM·BF_4/SWCNTs/CFUME, the much higher cathodic current of HRP-BMIM·BF_4/SWCNTs/CFUME indicated that HRP greatly promoted the catalytic reduction of H_2O_2. Moreover, HRP-BMIN·BF_4/SWCNTs/CFUME exhibited a much higher response to changes in the reduction peak current than HRP/SWCNTs/CFUME. Compared to the direct electrochemical reduction of H_2O_2 by the HRP/SWCNTs/CFUME (from approximately −0.2 V, curve b in Fig. 3B), the HRP-BMIN·BF_4/SWCNTs/CFUME reduced the reduction onset potential of H_2O_2 by at least 0.4 V (from approximately +0.2 V, curve b in Fig. 3A). The experimental results indicate that HRP retains its excellent bioactivity in the HRP-BMIM·BF_4/SWCNTs/CFUME. Additionally, these results indicate that BMIM·BF_4 absorbed on SWCNTs also contributes to the electrochemical reduction of H_2O_2 by HRP-BMIM·BF_4/SWCNTs/CFUME. The good conductivity of BMIM·BF_4 facilitates electron transfer in the three-dimensional HRP-BMIM·BF_4/SWCNTs film. Thus, the HRP-BMIM·BF_4/SWCNTs/CFUME has better bioelectrocatalytic activity than HRP/SWCNTs/CFUME toward H_2O_2.

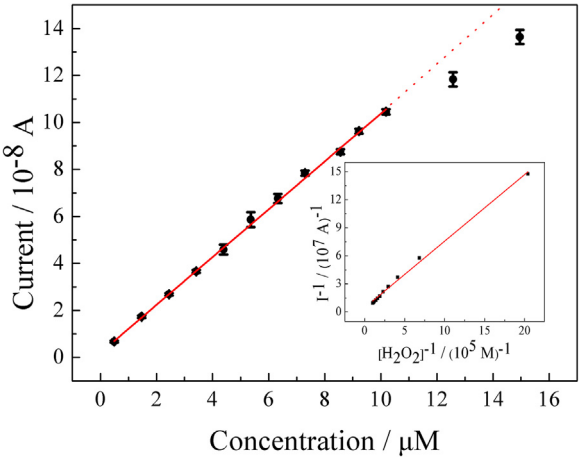

Fig. 4. Calibration curve of the faradic current to the concentration of H_2O_2 in air-saturated 0.01 M PBS buffer. Inset: the Lineweaver-Burk plot. Applied potential: −0.35 V vs. Ag/AgCl sat. KCl.

The dependence of the catalytic current on the addition of H_2O_2 is shown in Fig. S3. The enzyme electrode reached 95% of the steady state current within 6 s, suggesting that the response of the electrode to H_2O_2 should be a quick responsive process [22]. The linear range of H_2O_2 was from 0.49 μM to 10.2 μM (R^2 = 0.999; p = 3.7 e^{-14}) with a sensitivity of 4.25 A/M cm^2, and the detection limit was 0.13 μM at a signal-to-noise ratio of 3, according to the calibration curve presented in Fig. 4. The apparent Michaelis-Menten constant ($K_{m,app}$), which is an indicator of the affinity between the enzyme and substrate, can be derived from the modified Lineweaver–Burk equation $1/I_{ss} = (K_{m,app}/I_{max})(1/C) + (1/I_{max})$, where I_{ss} is the steady-state current after the addition of substrate, C is the bulk concentration of the substrate, and I_{max} is the maximum current measured under saturated substrate conditions. The $K_{m,app}$ was determined by analysis of the slope and intercept for the plot of the reciprocals of the steady state current

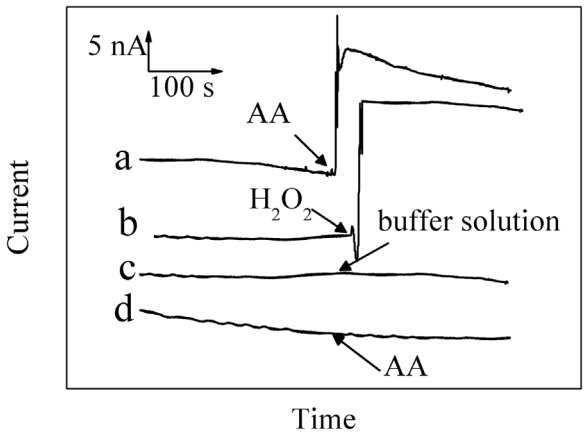

Fig. 5. Amperometric responses of the HRP-BMIM·BF_4/SWCNTs/CFUME for H_2O_2 released from HeLa cells after addition of 5 μM AA (a), HeLa cells after addition of 1.4 μM H_2O_2 (b), HeLa cells after addition of PBS alone (c), and PBS alone with addition of 5 μM AA (d).

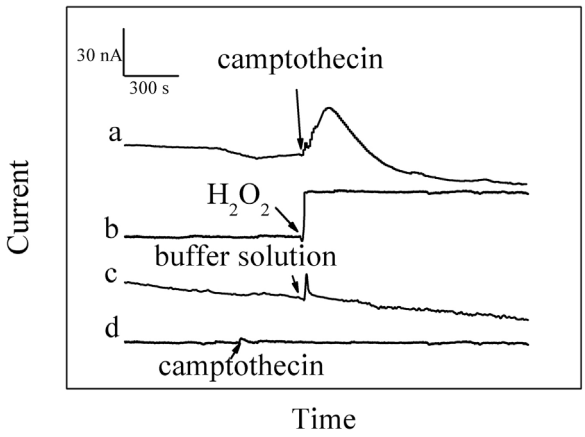

Fig. 6. Amperometric responses of the HRP-BMIM·BF_4/SWCNTs/CFUME for H_2O_2 released from HeLa cells after addition of 5 μM camptothecin (a), HeLa cells after addition of 2.7 μM H_2O_2 (b), HeLa cells after addition of PBS alone (c), and PBS alone with addition of 5 μM camptothecin (d).

versus H_2O_2 concentration. The smaller $K_{m,app}$ value represents a higher enzyme affinity for H_2O_2 [23]. From the Lineweaver–Burk plot in Fig. 4 inset, the $K_{m,app}$ value of the H_2O_2 sensor was 15.4 μM, which is much smaller than the values of the HRP-SG/CNT/GC electrode (1.35 mM) [24], HRP/Tb-MWCNT-modified graphite electrode (0.16 mM), MB-HRP/NME/MWCNTs/GC electrode (0.12 mM), and HRP/SGCCN film-modified GC electrode (23.85 mM) [25]. These results suggest that HRP molecules entrapped in the BMIM·BF_4 and SWCNTs immobilized at the carbon fiber ultramicroelectrode present high affinity.

In addition, the long-term stability of HRP-BMIM·BF_4/SWCNTs/CFUME was investigated. There was nearly no decrease in the H_2O_2 catalytic current after the modified electrode was maintained for 10 days at 4 °C. The long lifetime of the biosensor may be attributed to the biocompatibility and stability of the HRP-BMIM·BF_4/SWCNTs film [25]. This feature is ideal for *in vivo* real-time detection.

The reproducibility of the HRP-BMIM·BF_4/SWCNTs/CFUME was also investigated. The electrode-to-electrode reproducibility was characterized by a low relative standard deviation (R.S.D.) of 4.8% (n = 5) in response to 0.98 μM H_2O_2. The R.S.D. of 1.5% (n = 5) for 0.98 μM H_2O_2 obtained using the same electrode demonstrated good intra-electrode reproducibility.

3.4. Real-time in vitro detection of H_2O_2 released from HeLa cells

The HRP-BMIM·BF_4/SWCNTs/CFUME was used for the real-time *in vitro* detection of H_2O_2 in cells. HeLa cells, which generate H_2O_2 endogenously under AA stimulation, were chosen as model cells to demonstrate the electrochemical detection ability of the HRP-BMIM·BF_4/SWCNTs/CFUME. Before detection, HeLa cells were grown at 37 °C in 5% CO_2 in 25-cm^2 flasks containing Dulbecco's modified Eagle medium with 10% fetal bovine serum and 1% antibiotics. The culture medium was removed and the cells were washed three times with PBS, and then 1 mL of PBS containing 50 mM glucose was added for electrochemical measurements (as shown in Fig. S5). Without AA stimulation, these cells generated no measurable signal. Upon the addition of 5 μM AA, a significant increase in currents was observed (Fig. 5a). The maximum current change was approximately 16.3 nA, corresponding to 1.4 μM H_2O_2 as calculated from the calibration curve in Fig. 4. The current change was equal to that obtained by injecting 1.4 μM H_2O_2 in PBS in the HeLa cell culture (Fig. 5b). The current decreased gradually, indicating that H_2O_2 was either consumed or diffused away from the electrode surface. As controls, the currents were also measured when PBS without AA was injected on the HeLa cell culture (Fig. 5c) and when AA was injected in PBS alone (Fig. 5d), and no current change was observed. These results suggest that the HRP-BMIM·BF_4/SWCNTs/CFUME could be used for detection of H_2O_2 released from cells and that its potential functions could be exploited for physiological and pathological studies.

The HRP-BMIM·BF_4/SWCNTs/CFUME was also applied to detect the H_2O_2 increase in HeLa cells under injection of camptothecin in real-time. Camptothecin-induced generation of H_2O_2 is mediated by NADPH oxidase, which is activated by caspase-3(-like) proteases [26]. After a steady state background was attained, 5 μM camptothecin was injected into the solution. As shown in Fig. 6a, after injection of camptothecin, the current significantly increased and reached a maximum value of 29.5 nA at 2.5 min. The corresponding H_2O_2 concentration was 2.70 μM, and the current then decreased slowly to the baseline after 10 min, which was consistent with previous reports [27,28]. The effluxed H_2O_2 may re-enter the cells or may be scavenged by secreted enzymes [29,30]. The peak value of the current response indicates the maximum H_2O_2 efflux. The current change was equal to that observed after injecting 2.7 μM H_2O_2 in PBS to the HeLa cell culture (Fig. 6b). As controls, the currents were also measured when injecting PBS without camptothecin into the HeLa cell culture (Fig. 6c) and when injecting camptothecin in PBS alone (Fig. 6d), and no current change was observed.

In this study, the HRP-BMIM·BF_4/SWCNTs/CFUME was first placed in cells that adhered to the dish and a potential of −0.35 V was applied. After a steady state background was obtained, 50 μM AA or camptothecin was injected into the buffer. The experiments were repeated more than 10 times. A significant increase in the currents was observed less than 10 s after AA addition, and the interval time between current increase and camptothecin addition was 10 ± 1 min, which was consistent with previous research [31,32]. This biosensor is the first to use carbon fiber modified with enzymes coupled with CNTs and ionic liquid to detect H_2O_2 released by cancer cells under camptothecin stress. When compared with similar sensors, the sensor used in this study achieved better results in terms of the limit of detection (Table 1) [33–38]. However, limitations exist in the use of HRP-BMIM·BF_4/SWCNTs/CFUMEs. The electrode was not small enough to detect H_2O_2 in a single cell. The electrochemical data in this study provided the relative change of cellular H_2O_2 under camptothecin stress, but not the absolute cellular H_2O_2 content. In the future, the carbon fiber electrode should be etched in the nanometer range for *in vivo* applications.

Table 1
Comparison of analytical the performance of H_2O_2 biosensors.

H_2O_2 biosensor	Detection limit (μM)	Refs.
HRP-BMIM·BF_4/SWCNTs	0.13	This work
HRP-AuNP-PEG	1	[33]
HRP/TTF–TCNQ/MWCNTs	0.5	[34]
Hb/SWCNTs	4	[35]
HAP-α-zirconium phosphate/GC	1.2	[36]
HRP-nano-Au-carbon ceramic	6.1	[37]
HRP-DNA/GC	0.3	[38]

4. Conclusion

HRP-BMIM·BF_4/SWCNTs/CFUME was successfully fabricated and employed for electrochemical monitoring of the cellular H_2O_2 level under camptothecin stress in real-time *in vitro*. The electrochemical data suggest that HRP retained its catalytic activity and reduced H_2O_2 after being immobilized on SWCNT-coated CFUME. SWCNTs immobilized on the CFUME surface greatly increased the specific surface area for HRP and BMIM·BF_4 immobilization. SWCNTs and BMIM·BF_4 facilitated electron transfer of HRP to improve the detection limit and resulted in a favorable anti-interference ability and highly selective detection of H_2O_2 without incorporating a redox mediator or extra anti-interference coatings. Moreover, the biocompatibility and stability of the HRP-BMIM·BF_4/SWCNTs film provide the biosensor with a long lifetime. These features are especially preferred for a biosensor. The HRP-BMIM·BF_4/SWCNTs/CFUME was successfully applied to real-time detection of cellular H_2O_2 under camptothecin stress and generated straightforward amperometric data. This real-time cellular H_2O_2 sensor is expected to facilitate research on the role of H_2O_2 in the occurrence, development, and apoptosis of tumors.

Fundings

This study was supported by the National Natural Science Foundation of China (Grant no. 61305147), the Natural Science Foundation of HeNan Province (Grant nos. 16A416009, 2014 GGJS-096, 17A535003, 152102310357), and the support project for the Disciplinary group of Psychology and Neuroscience, Xinxiang Medical University (2016PN-KFKT-24).

Acknowledgements

We would like to thank Editage [www.editage.cn] for English language editing. We also thank the Analytical and Testing Center (HUST) for help with measurement.

Appendix A. Supplementary data

Supplementary data associated with this article can be found, in the online version, at http://dx.doi.org/10.1016/j.snb.2017.02.001.

References

[1] S. Kawanishi, Y. Hiraku, S. Pinlaor, N. Ma, Oxidative and nitrative DNA damage in animals and patients with inflammatory diseases in relation to inflammation-related carcinogenesis, Biol. Chem. 387 (2006) 365–372.
[2] M.L. Heaney, J.R. Gardner, N. Karasavvas, D.W. Golde, D.A. Scheinberg, E.A. Smith, et al., Vitamin C antagonizes the cytotoxic effects of antineoplastic drugs, Cancer Res. 68 (2008) 8031–8038.
[3] J. Song, J. Li, J. Qiao, S. Jain, B. Mark Evers, D.H. Chung, PKD prevents H_2O_2-induced apoptosis via NF-κB and p38 MAPK in RIE-1 cells, Biochem. Biophys. Res. Commun. 378 (2009) 610–614.
[4] J. Alexandre, F. Batteux, C. Nicco, C. Chereau, A. Laurent, L. Guillevin, et al., Accumulation of hydrogen peroxide is an early and crucial step for paclitaxel-induced cancer cell death both in vitro and in vivo, Int. J. Cancer 119 (2006) 41–48.
[5] C. Lu, G. Song, J.M. Lin, Reactive oxygen species and their chemiluminescence-detection methods, Trac Trends Anal. Chem. 25 (2006) 985–995.
[6] M. Liu, B.X. Li, X. Cui, Anionic polythiophene derivative as peroxidase mimetics and their application for detection of hydrogen peroxide and glucose, Talanta 115 (2013) 837–841.
[7] D.P. Murale, H. Liew, Y.H. Suh, D.G. Churchill, Mercuric-triggered hydrogen peroxide turn-on fluorescence detection in neuronal cells with novel fluorescein-based probe obtained in one pot, Anal. Methods 5 (2013) 2650–2652.
[8] Q.Q. Ren, X.R. Huang, G.C. Liu, J. Ou-Yang, M.T. Li, H. Chen, et al., A field-compatible technique using an electrochemical sensing microbundle for real-time and simultaneous in vivo measurement of hydrogen peroxide, nitric oxide, and pH under drought stress, Sens. Actuators B Chem. 220 (2015) 743–748.
[9] M.L. Huffman, B.J. Venton, Carbon-fiber microelectrodes for in vivo applications, Analyst 134 (2009) 18–24.
[10] Q.Q. Ren, X.J. Yuan, X.R. Huang, W. Wen, Y.D. Zhao, W. Chen, In vivo monitoring of oxidative burst on aloe under salinity stress using hemoglobin and single-walled carbon nanotubes modified carbon fiber ultramicroelectrode, Biosens. Bioelectron. 50 (2013) 318–324.
[11] S. Huang, L.M. Wang, C.S. Huang, W. Su, Q. Xiao, Amino-functionalized graphene quantum dots based ratiometric fluorescent nanosensor for ultrasensitive and highly selective recognition of horseradish peroxidase, Sens. Actuators B Chem. 234 (2016) 255–263.
[12] Y.H. Wu, Q.C. Shen, S.S. Hu, Direct electrochemistry and electrocatalysis of heme-proteins in regenerated silk fibroin film, Anal. Chim. Acta 558 (2006) 179–186.
[13] J.Q. Sun, B.F. Ye, G.M. Xia, X.H. Zhao, H.M. Wang, A colorimetric and fluorescent chemosensor for the highly sensitive detection of CO_2 gas: experiment and DFT calculation, Sens. Actuators B Chem. 233 (2016) 76–82.
[14] Q.L. Sheng, J.B. Zheng, X.D. Shang-Guan, W.H. Lin, Y.Y. Li, R.X. Liu, Direct electrochemistry and electrocatalysis of heme-proteins immobilized in porous carbon nanofiber/room-temperature ionic liquid composite film, Electrochim. Acta 55 (2010) 3185–3191.
[15] S. Park, R.J. Kazlauskas, Biocatalysis in ionic liquids–advantages beyond green technology, Curr. Opin. Biotechnol. 14 (2003) 432–437.
[16] Q. Chen, M.G. Espey, M.C. Krishna, J.B. Mitchell, C.P. Corpe, G.R. Buettner, et al., Pharmacologic ascorbic acid concentrations selectively kill cancer cells: action as a pro-drug to deliver hydrogen peroxide to tissues, Proc. Natl. Acad. Sci. U. S. A. 102 (2005) 13604–13609.
[17] A.M. Strand, B.J. Venton, Flame etching enhances the sensitivity of carbon-fiber microelectrodes, Anal. Chem. 80 (2008) 3708–3715.
[18] H.A. Rafiee-Pour, M. Hamadanian, S.K. Koushali, Nanocrystalline TiO_2 films containing sulfur and gold: synthesis, characterization and application to immobilize and direct electrochemistry of cytochrome c, Appl. Surf. Sci. 363 (2016) 604–612.
[19] S. Palanisamy, Y.T. Wang, S.M. Chen, B. Thirumalraj, B.S. Lou, Direct electrochemistry of immobilized hemoglobin and sensing of bromate at a glassy carbon electrode modified with graphene and beta-cyclodextrin, Microchim. Acta. 183 (2016) 1953–1961.
[20] Y.M. Yan, W. Zheng, M.N. Zhang, L. Wang, L. Su, L.Q. Mao, Bioelectrochemically functional nanohybrids through co-assembling of proteins and surfactants onto carbon nanotubes: facilitated electron transfer of assembled proteins with enhanced faradic response, Langmuir 21 (2005) 6560–6566.
[21] X.B. Lu, Q. Zhang, L. Zhang, J.H. Li, Direct electron transfer of horseradish peroxidase and its biosensor based on chitosan and room temperature ionic liquid, Electrochem. Commun. 8 (2006) 874–878.
[22] C. Xiang, Y. Zou, L.-X. Sun, F. Xu, Direct electron transfer of cytochrome c and its biosensor based on gold nanoparticles/room temperature ionic liquid/carbon nanotubes composite film, Electrochem. Commun. 10 (2008) 38–41.
[23] Y. Lu, W.C. Ye, Q. Yang, J. Yu, Q. Wang, P.P. Zhou, et al., Three-dimensional hierarchical porous PtCu dendrites: a highly efficient peroxidase nanozyme for colorimetric detection of H_2O_2, Sens. Actuators B Chem. 230 (2016) 721–730.
[24] J.W. Wang, M. Gu, J.W. Di, Y.S. Gao, Y. Wu, Y.F. Tu, A carbon nanotube/silica sol-gel architecture for immobilization of horseradish peroxidase for electrochemical biosensor, Bioprocess Biosyst. Eng. 30 (2007) 289–296.
[25] H.J. Chen, S.J. Dong, Direct electrochemistry and electrocatalysis of horseradish peroxidase immobilized in sol-gel-derived ceramic-carbon nanotube nanocomposite film, Biosens. Bioelectron. 22 (2007) 1811–1815.
[26] S. Simizu, M. Takada, K. Umezawa, M. Imoto, Requirement of caspase-3(-like) protease-mediated hydrogen peroxide production for apoptosis induced by various anticancer drugs, J. Biol. Chem. 273 (1998) 26900–26907.
[27] B. Liu, D.L. Wang, Y.K. Liu, Q. Zhang, L.L. Meng, H.R. Chi, et al., Hydrogen peroxide-responsive anticancer hyperbranched polymer micelles for enhanced cell apoptosis, Polym. Chem. 6 (2015) 3460–3471.
[28] C. Zhang, S.H. Chen, J.L. Bao, Y.L. Zhang, B.R. Huang, X.J. Jia, et al., Low doses of camptothecin induced hormetic and neuroprotective effects in PC12Cells, Dose Response 13 (2015).
[29] M. López-Lázaro, Dual role of hydrogen peroxide in cancer: possible relevance to cancer chemoprevention and therapy, Cancer Lett. 252 (2007) 1–8.
[30] D. Trachootham, J. Alexandre, P. Huang, Targeting cancer cells by ROS-mediated mechanisms: a radical therapeutic approach? Nat. Rev. Drug Discov. 8 (2009) 579–591.

[31] C. Yu, Z. Zhu, Q. Wang, W. Gu, N. Bao, H. Gu, A disposable indium-tin-oxide sensor modified by gold nanorod-chitosan nanocomposites for the detection of H2O2 in cancer cells, Chem. Commun. 50 (2014) 7329–7331.
[32] Y. Zhang, X. Bai, X. Wang, K.-K. Shiu, Y. Zhu, H. Jiang, Highly sensitive Graphene–Pt nanocomposites amperometric biosensor and its application in living cell H_2O_2 detection, Anal. Chem. 86 (2014) 9459–9465.
[33] B.P. Crulhas, N.P. Ramos, G.R. Castro, V.A. Pedrosa, Detection of hydrogen peroxide releasing from prostate cancer cell using a biosensor, J. Solid State Electrochem. 20 (2016) 2427–2433.
[34] Z. Cao, X. Jiang, Q. Xie, S. Yao, A third-generation hydrogen peroxide biosensor based on horseradish peroxidase immobilized in a tetrathiafulvalene–tetracyanoquinodimethane/multiwalled carbon nanotubes film, Biosens. Bioelectron. 24 (2008) 222–227.
[35] Q.-Q. Ren, X.-J. Yuan, X.-R. Huang, W. Wen, Y.-D. Zhao, W. Chen, In vivo monitoring of oxidative burst on aloe under salinity stress using hemoglobin and single-walled carbon nanotubes modified carbon fiber ultramicroelectrode, Biosens. Bioelectron. 50 (2013) 318–324.
[36] X. Yang, X. Chen, L. Yang, W. Yang, Direct electrochemistry and electrocatalysis of horseradish peroxidase in α-zirconium phosphate nanosheet film, Bioelectrochemistry 74 (2008) 90–95.
[37] C.-X. Lei, S.-Q. Hu, N. Gao, G.-L. Shen, R.-Q. Yu, An amperometric hydrogen peroxide biosensor based on immobilizing horseradish peroxidase to a nano-Au monolayer supported by sol–gel derived carbon ceramic electrode, Bioelectrochemistry 65 (2004) 33–39.
[38] X. Zeng, X. Li, X. Liu, Y. Liu, S. Luo, B. Kong, et al., A third-generation hydrogen peroxide biosensor based on horseradish peroxidase immobilized on DNA functionalized carbon nanotubes, Biosens. Bioelectron. 25 (2009) 896–900.

Biographies

Qiong-Qiong Ren gained her BA degree from College of Life Science and Technology-Huazhong University of Science and Technology, P. R. China in 2010, and Ph.D degree in the same school in 2015. At present, she is a lecturer in Biomedical Engineering collage, Xinxiang Medical University, Xinxiang, China. Her current interest is in analytical electrochemistry and nanobiosensor.

Jing Wu gains her BA degree in biological science from Henan Normal University in 2006 and PhD about Biochemistry and Molecular Biology in Huazhong University of Science & Technology. At present, she is a lecturer in Institute of Lung and Molecular Therapy, Xinxiang Medical University, Xinxiang, China. Her current research interest is the Molecular therapy methods and genetic factors in pulmonary diseases.

Wen-Chao Zhang gained his BA degree from Henan Normal University, P.R.China in 2005 and Post-Graduate from Nanjing University of Science and Technology, P.R.China in 2013. At present, he is a lecturer in XinXiang Medical University. His current research interest is serial mode in MRI.

Chang Wang obtained his BA degree from Xinxiang Medical university, P. R. China in 2007. He received his MA degree from University of Science and Technology of China, P. R. China in 2010. At present, He is a lecturer in Xinxiang Medical University. His research interest is in medical image processing and brain function analysis.

Xin Qin gained her BS degree from University of Jinan in 2003. At present, she is an asssociate professor in Institute of Biomedical engineering, Xinxiang Medical University. Her current research interest is Biomedical engineering.

Guo-Chang Liu is studying his Master degree in College of Life Science and Technology-Huazhong University of Science and Technology, P. R. China. His current interest is in electrochemical biosensors.

Zhen-Xin Li gained his BA degree from Henan Normal University, P.R.China in 1987 and Ph. D from school of materials science and engineering-Wuhan University of Technology, P. R. China in 2006. At present, he is a professor in Biomedical Engineering collage, Xinxiang Medical University, Xinxiang, China. His current interest is in material physical properties and biological sensors.

Yi Yu gained his BA degree from School of Information and Electrical Engineering-Shandong University of Science and Technology in 2005 and Ph. D from institute of biomedical engineering and instrument science-Zhejiang University in 2010. At present, he is an associate professor in Biomedical Engineering collage, Xinxiang Medical University, Xinxiang, China. His current interest is in neural sensing and control engineering and medical information processing.